

Copyright Warning & Restrictions

The copyright law of the United States (Title 17, United States Code) governs the making of photocopies or other reproductions of copyrighted material.

Under certain conditions specified in the law, libraries and archives are authorized to furnish a photocopy or other reproduction. One of these specified conditions is that the photocopy or reproduction is not to be “used for any purpose other than private study, scholarship, or research.” If a user makes a request for, or later uses, a photocopy or reproduction for purposes in excess of “fair use” that user may be liable for copyright infringement,

This institution reserves the right to refuse to accept a copying order if, in its judgment, fulfillment of the order would involve violation of copyright law.

Please Note: The author retains the copyright while the New Jersey Institute of Technology reserves the right to distribute this thesis or dissertation

Printing note: If you do not wish to print this page, then select “Pages from: first page # to: last page #” on the print dialog screen

The Van Houten library has removed some of the personal information and all signatures from the approval page and biographical sketches of theses and dissertations in order to protect the identity of NJIT graduates and faculty.

ABSTRACT
Bead Design for
Effect of 2,3-Butanedione
Monoxime on Whole-Cell Potassium
Channel Current in Rat Single Myocytes

by
Youliang Zhou

The patch clamp technique is a simple procedure which can isolate ion channels on cell membranes. Our previous data have shown that 2,3-Butanedione Monoxime (BDM) could inhibit the calcium current by dephosphorylation of the channel. In this study, the effect of BDM on the potassium channels were investigated with the whole-cell recording method in single myocytes enzymatically isolated from the left ventricle of 3-4 months old rats. Superfusion of myocytes with BDM elicited a dose dependent decrease of the outward transient potassium current. BDM with concentrations of 5, 20 and 50 mM reduced the maximal peak potassium current by $7.3 \pm 2.3\%$, $68.7 \pm 6.1\%$ and 100%. 5 μM of isoproterenol (Iso) partially reversed the inhibitory action of 20 mM BDM on potassium current. Furthermore, 2 μM of isoproterenol (Iso) applied to bath solution without BDM could enhance the peak potassium current about 15%. Our present data suggest that BDM and Iso can either inhibit or enhance the potassium current by dephosphorylation or phosphorylation of the potassium channels.

EFFECT OF 2,3-BUTANEDIONE
MONOXIME ON WHOLE-CELL
POTASSIUM CHANNEL CURRENTS IN
RAT SINGLE MYOCYTES

by
Youliang Zhou

A Thesis
Submitted to the Faculty of the
New Jersey Institute of Technology
in Partial Fulfillment of the Requirements for the Degree of
Master of Science
in Biomedical Engineering
May 1992

APPROVAL PAGE
Bead Design for
Effect of 2,3-Butanedione
Monoxime on Whole-Cell
Potassium Channel Currents in
Rat Single Myocytes

by
Youliang Zhou

5/11/92

Dr. Peter Engler, Thesis Adviser

Associate Professor of Electrical and Computer Engineering, NJIT

5/11/92

Dr. David Kristol, Committee member

Director and Professor of Biomedical Engineering, NJIT

5/13/92

Dr. Joseph J. McArdle, committee member

Professor of Pharmacology, UMDNJ

BIOGRAPHICAL SKETCH

Author: Youliang Zhou

Degree: Master of Science in Biomedical Engineering

Date: May, 1988

Date of Birth:

Place of Birth:

Undergraduate and Graduate Education:

- Master of Science in Biomedical Engineering, New Jersey Institute of Technology, Newark, NJ, 1992
- Bachelor of Science in Biomedical Engineering, Shanghai Medical University, Shanghai, P. R. China, 1985

Major: Biomedical Engineering

ACKNOWLEDGEMENT

I am deeply indebted to my primary thesis advisor Dr. Peter Engler for his expert guidance and assistance. His constant encouragement and thoroughness contributed toward the completion of this thesis. Special thanks are also due to my other advisors, Dr. David Kristol and Joseph J. McArdle, for their advice, support and encouragement. All the work was done under the assistance of Dr. Yongfu Xiao who worked with me and provided technical support towards the operation of the patch clamp equipment.

TABLE OF CONTENTS

	Page
1 INTRODUCTION	1
2 BASIC PRINCIPLE	5
2.1 Physiological Aspects.....	5
2.2 Electronics for Whole-cell Clamping.....	9
2.2.1 Current-Voltage converter.....	9
2.2.2 Capacitance Transient Cancellation.....	9
2.2.3 Series Resistance Compensation.....	13
2.3 Pipettes.....	14
2.4 Enzymatic Dispersion of Heart Tissues.....	16
3 METHODS	19
3.1 Animal.....	19
3.2 Single-cell Isolation.....	19
3.3 Electrophysiological Recording.....	20
3.4 Solution.....	21
3.5 Cell Capacity and Series Resistance.....	22
3.6 Voltage Protocol and Analysis of Membrane Current.....	24
4 RESULTS	25
5 DISCUSSIONS AND CONCLUSIONS.....	44
REFERENCES.....	46

LIST OF FIGURES

Figure	Page
1 Outline of Seal Between Pipette and Membrane.....	4
2 Model of Na ⁺ and K ⁺ Contribution to Membrane Potential.....	7
3 Outline of Pipette.....	10
4 Current Activated in a 10 mV Hyperpolarizing Pulse from a Holding Potential of -80 mV.....	12
5 Current-voltage Converter Circuit.....	15
6 Circuit of Capacitance Cancellation.....	17
7 Circuit of Series Resistance Compensation.....	23
8 Outward Transient Potassium Current Activated in 10 mV Increments from -80 to 60 mV in Normal Bath Solution.....	26
9 Outward Transient Potassium Current Activated in 10 mV Increments from -80 to 60 mV after 10 min Wash-in of 20 mM of BDM.....	27
10 Outward Transient Potassium Current Activated in 10 mV Increments from -80 to 60 mV after 10 min Wash-in of 50 mM of BDM.....	28
11 Washout Current Records.....	30
12 Voltage Dependence of Outward Transient Potassium Current in the Absence and Presence of 20 mM BDM.....	31
13 The Time Constant Curve in the Absence and Presence of 20 mM BDM.....	32
14 Membrane Current Activated in 10 mV Increments from -80 to 60 mV in Normal Bath Solution.....	33
15 Membrane Current Activated in 10 mV increments from -80 to 60 mV after 10 min Wash-in of 5 μ M of Iso.....	34
16 Partial Reverse Effect of Iso.....	37
17 BDM Dose-dependent Curve.....	38

18 Dose-dependent Curve of the Effect of BDM on the Peak Current and Steady-state Current.....	39
19 Dose-dependent Curve of the Effect of BDM on the Single Exponential Time of Decay Rate.....	40
20 Inactivation Curve of Outward Transient Potassium Current Examined in the Absence of BDM.....	41
21 Inactivation Curve of Membrane Current Examined in the Presence of 20 mM BDM.....	42
22 Inactivation Curve of Membrane Current Examined after 10 min of Normal Bath Solution.....	43

1 INTRODUCTION

2,3-Butanedione Monoxime (BDM), a member of the oxime family, has been reported to depress twitch and tetanic contractions in skeletal muscle and have a negative inotropic (influencing muscular contractility) action in cardiac muscle. A lot of work has been done on the effect of BDM on the calcium channel. A number of sites of action have been proposed; For example concentrations of $BDM < 2mM$ inhibited the release of Ca^{2+} from intracellular stores in mammalian skeletal muscle, but not in cardiac muscle or frog skeletal fibres (Blanchard, Alpert, Allen and Smith, 1988; Fryer, Gage, Neering, Dulhunty and Lamb, 1988; Fryer, Neering and Stephenson, 1988b; Maylie and Hui, 1988). At high concentrations, BDM (2-10mM) decreased the sensitivity of the contractile apparatus to Ca^{2+} (Li, Sperelakis, Teneick and Solaro, 1985; Fryer et al, 1988) and modified the number of interacting cross bridges (Blanchard et al, 1988). The duration of the action potentials in cardiac muscle and the Ca^{2+} current in skeletal muscle were also reduced by these high concentrations of BDM (Bergey, Reiser, Wiggins and Freeman, 1981; Fryer et al, 1988). The tonic contraction of the rat anococcygeus (a muscle arising from the ligament and inserted into the sacrum in anus), to raised external concentrations of potassium or phenylephrine, was inhibited by BDM (5-30mM) to a greater extent than the phasic component (normal component). In single ureteral rat cells bathed in Ba^{2+} -containing solutions, BDM (5-20mM) reduced the duration of action potentials and Ca^{2+} channel

currents recorded under voltage-clamp conditions (Lang and Wendit, 1987). As oximes are mild nucleophilic agents, which can reactivate cholinesterase poisoned with organophosphorous groups, it has been suggested BDM has a phosphatase-like activity and, as such, may prove a useful tool with which to study K^+ channel function in rat single myocytes. Little has been done on the effect of BDM on potassium channels, so we chose this study as our research topic.

The duration of the action potential plateau is in part regulated by modulation of potassium (K^+) current in rat ventricular myocytes and the time-dependent delayed rectifier (a kind of potassium current which has the characteristics of a rectifier) K^+ currents are the most prominent time-dependent potassium efflux pathways. The potassium currents appear to be the major current activated at plateau potentials in both the rat ventricle and in most mammalian atrial tissues, including the human atrial tissues (Escande et al, 1987). In other mammalian ventricular tissues, the most significant time-dependent outward current is the potassium current (Jewell, 1981), that is modulated by catecholamines (Walsh and Kass, 1988). Since a change of potassium current would result in the change of the duration of the action potential, we measured the effect of BDM on the K^+ channels in single rat ventricular myocytes for a deeper understanding of the characteristics of action potential.

Although patch pipettes were originally developed for the recording of single channels, they can be of great advantage for more conventional recordings from whole cells, particularly when the cells under study are small.

A membrane patch can be broken by a short pulse of suction after a gigaseal (high pipette-membrane seal resistance of 20 G ohm as shown in figure 1) has been formed. Very often, this manipulation does not damage the pipette-membrane seal, so that a conductive pathway is established between the pipette and the cell interior, which is well insulated from the bath. It is our experience that this method of penetrating a cell inflicts much less damage on the cell than the standard microelectrode impalement. If small cells are used, their input resistance (series resistance plus membrane resistance) is very large compared to the access resistance of the pipette tip, so that meaningful electrical measurement may be performed even though the signal originates from a much larger membrane area than that of the initial patch. This method is called "whole-cell recording". We used this method in all our experiments.

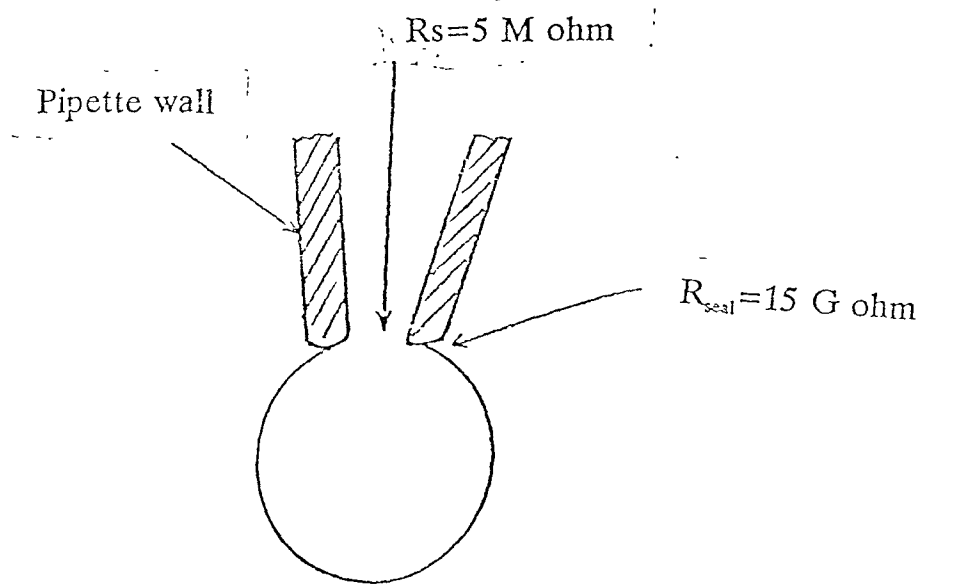


Figure 1 Outline of seal between pipette and membrane

2 BASIC PRINCIPLE

2.1 Physiological Aspects

It has been recognized for more than a century that the muscle impulse is an electrical phenomenon. A clear picture of the mechanism of the action potential was not developed, however, until critical experiments were made possible by intracellular recording techniques, which were introduced independently in 1939-1940 by Cole and Curtis in the U. S .A and by Hodgkin and Huxley in England. Muscle cells and nerve cells maintain a steady potential (inside negative) across their membranes. This steady potential is usually referred to as the resting potential. When a sufficiently strong, brief electric current is passed outward through the membrane of an axon or a muscle cell, the membrane potential undergoes a unique sequence of changes which is peculiar to excitable cells. This sequence constitutes the action potential which has threshold, all-or-nothing characteristics.

If a membrane is permeable only to K^+ ions, for example, and if there is a concentration gradient of K^+ across the membrane, the diffusion of K^+ through the membrane is self-limiting. The first K^+ ions to penetrate the membrane generate an electric field which retards the diffusion of other K^+ ions. As long as there is a net outflux of K^+ , positive and negative charges are being separated and the electric field is increasing, so that eventually the electric field must attain a strength to permit influx to equal the outflux. If no work is needed to carry a small amount of a substance across the

transmembrane potential which equalizes fluxes for a particular ion is called the equilibrium potential. There is an equation to calculate this potential which is called the Nernst equation.

$$E_K = (RT/FZ_K) (\ln [K^+]_o / [K^+]_i)$$

where R: universal gas constant.

T: absolute temperature.

F: number of coulombs per mole of charge.

Z_K : the valence of ion.

$[K^+]_o$: concentration of K^+ outside.

$[K^+]_i$: concentration of K^+ inside.

The typical value of E_K and E_{Na} is -75 mV and 55 mV respectively. The membrane is an electrical capacitor because of its insulating, charge-separating properties, and has high a resistance because ions are able to penetrate it at a limited rate. An approximately equivalent circuit consisting of resistors, voltage sources and a capacitor can represent an electrical model of the cell membrane as in figure 2. A capacitor (C_m) represents the insulating charge-storing aspect of the membrane. E_{Na} and E_K are the Nernst potential of Na^+ and K^+ . g_{Na} and g_K are the conductance of Na^+ and K^+ representing the limited ability of ions to penetrate the membrane.

It is difficult to learn the detailed kinetics of an explosive process. A better way to study them is by controlling a variable so that threshold, all-or-nothing characteristics are eliminated. In muscle, the threshold behavior can be eliminated by "clamping" the voltage at values set by the experimenter. The relation between voltage across the membrane and membrane ionic

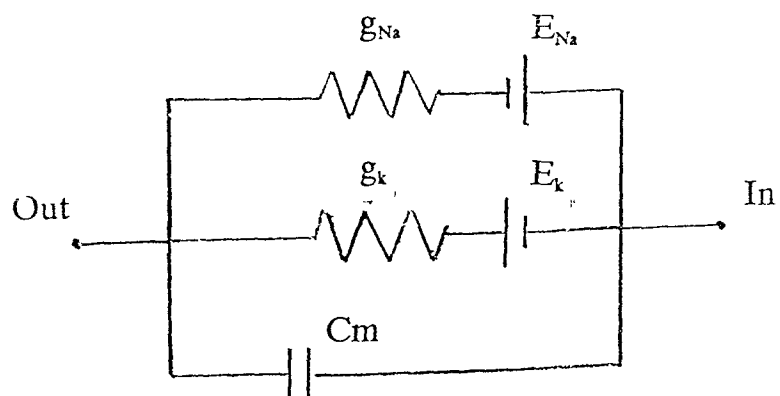


Figure 2 Model of Na^+ and K^+ contribution to membrane potential

current is measured by supplying to the muscle, from an external source, whatever current is required to maintain the membrane voltage constant-i.e., connecting it to a battery for different values of the voltage.

The total membrane current can be separated into sodium and potassium ion currents by analyzing the manner in which changes in concentration of sodium or concentration of potassium affect the shapes of curves relating current to time. It has been found that changes in concentration of sodium change sodium currents but not potassium currents. Thus the change in currents due to a change in concentration of sodium is carried by the sodium ion. The sodium currents rise rapidly along an S-curve, reaches a peak in about 0.5 millisecond and then declines to near zero in another 2 milliseconds, the potassium currents also rise along an S-curve, but much more slowly, and then level off at a high maintained value in about 4 milliseconds. If sodium ion and potassium ion components are correctly identified, the conductance of sodium ion (g_{Na}) and that of potassium ion (g_k) as a function of time can be determined by dividing the ionic current by the driving force (membrane potential minus Nernst potential) on that ion.

Thus $g_k = I_k / (E_m - E_k)$

and $g_{Na} = I_{Na} / (E_m - E_{Na})$

where E_m : Membrane potential

E_k : Nernst equivalent potential of potassium

E_{Na} : Nernst equivalent potential of sodium

I_k : Current of potassium

I_{Na} : Current of potassium

2.2 Electronics for Whole-cell Clamping

2.2.1 Current-Voltage Converter

Figure 3 shows the current-voltage converter circuit. The output voltage changes in response to differences in the voltage V_+ and V_- at the input terminals according to

$$dV_{out}/dt = W_a(V_+ - V_-)$$

The factor W_a can be very large: for typical commercial op-amps, it is about 10^7 sec^{-1} , which means that 1 mV difference on the input terminals causes the output voltage to slew at 10^4 V/sec . The op-amp varies its output to keep the pipette potential at V_{ref} . This action can be made very rapid and precise, so that for practical purposes V_p (potential of pipette) can be assumed to be precisely V_{ref} . This in turn allows us to measure $V_B - V_{ref}$ as shown, rather than $V_B - V_p$, to obtain the voltage drop across the resistor. The resistor R (typical value 20 G ohm) is made very large for high sensitivity. V_{ref} is the command potential V_{cmd} which is a rectangular waveform at the time of making a seal or different protocol at the time of testing. The voltage difference is usually measured using a standard differential amplifier circuit.

2.2.2 Capacitance Transient Cancellation

Step potential changes can be applied to membrane patches or to entire cells by applying a step command voltage as the reference voltage V_{ref} of the I-V converter. The converter in turn causes the pipette voltage to follow V_{ref} , forcing any necessary currents through the feedback resistor to bring V_p to the correct level. The currents that flow in charging the pipette capacitance C_p (the capacitance of the pipette wall: typically 2PF) are typically some

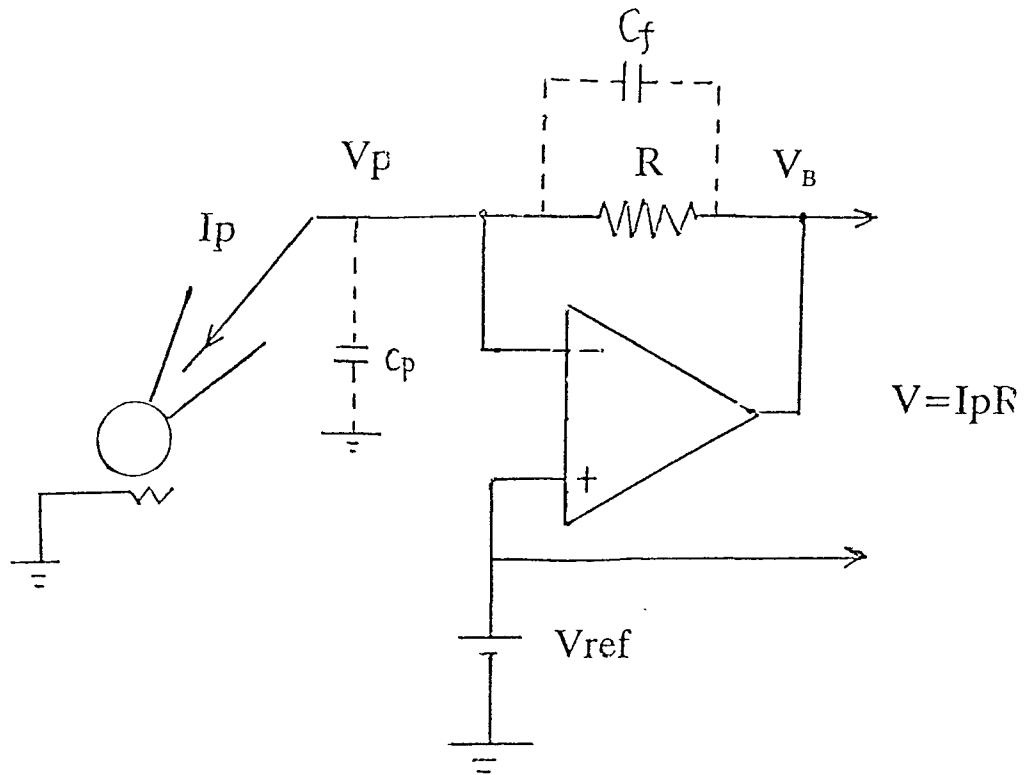


Figure 3 Current-voltage converter circuit

nanoamperes in magnitude, very large compared to the currents across the membrane. The large current causes two problems. First, they generally exceed the linear range of the recording device (e.g. A-D converter). This means that for a short interval after a voltage step, the membrane current information is lost. Second, if the membrane current pulse is large enough to drive amplifiers into saturation, serious distortions of the current monitor signal can persist even for several milliseconds after the current pulse is over.

The worst thing that can happen is that the I-V converter op-amp goes into saturation. Because no feedback is then possible, the pipette is no longer voltage clamped but sees the high impedance of the feedback resistor (R). The current monitor signal shows a large step-like response, the total duration of which equals the saturation time.

To determine whether a given voltage step will cause saturation, we notice first that the rapid charging currents will flow primarily through the stray capacitance C_f (capacitance of the feedback resistor R) rather than through the feedback resistor itself. The output voltage therefore shows an initial step of magnitude:

$$V_{out} = V_{ref} \left(\frac{C_p}{C_f} + 1 \right)$$

Slower currents, such as those arising in whole-cell clamp from the cell capacitance, must also be small enough to be passed through the feedback resistor (With a 10 G ohm feedback resistor and a 10 V maximum output voltage, the largest current that can be passed is 1 nA).

Figure 4 shows the circuit of capacitance cancellation. C_i is used for the cancellation of C_p , C_2 and R_2 is used for the cancellation of C_m . R_m is the

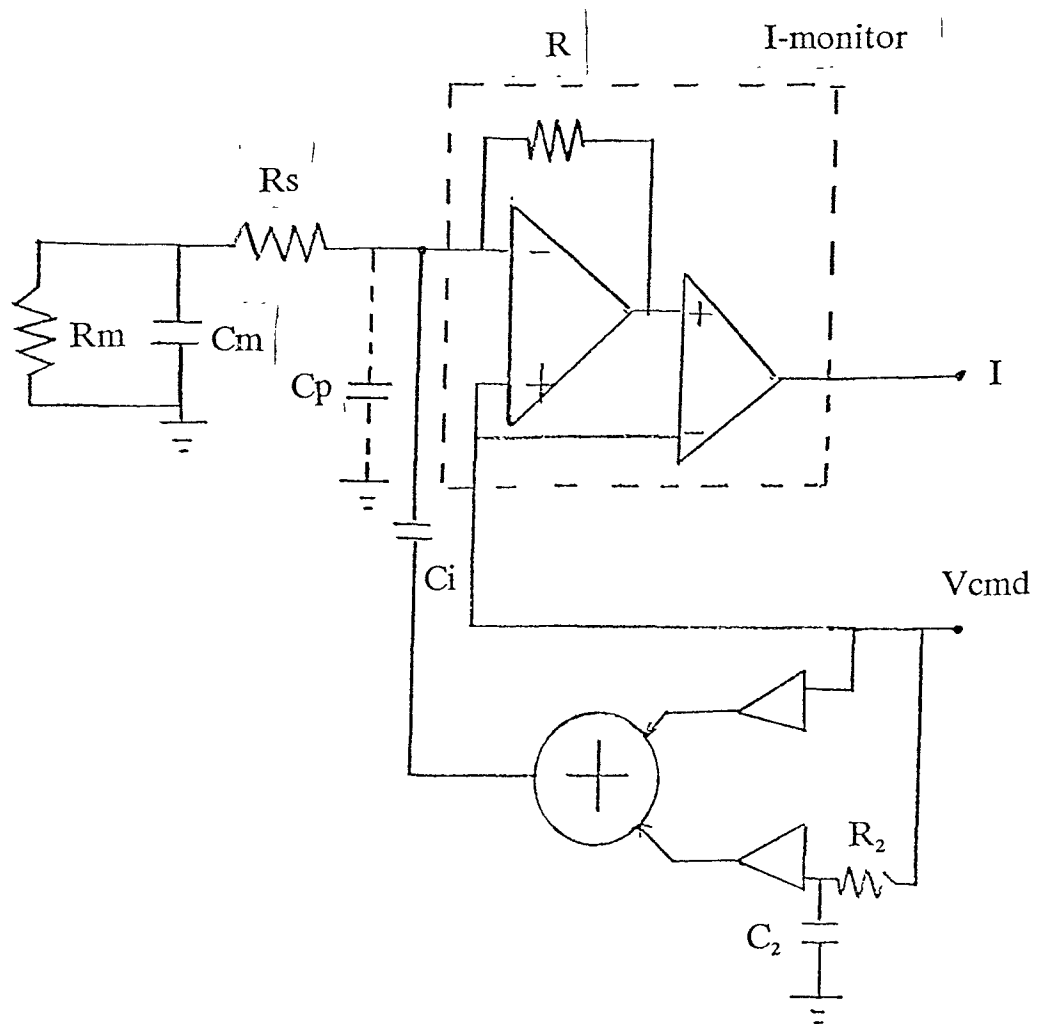


Figure 4 Circuit of capacitance cancellation

membrane resistance. C_m is the membrane capacitance.

When the command potential ($V_{cmd}=V_p$) changes, current I_p flows into C_p to charge it to the new potential. If no compensation is used, I_p is supplied by feedback resistor R resulting in a large transient signal on the output currents. By properly setting C_i and R_2 and C_2 , after amplification, the two signals are summed. In this case no current need be supplied by feedback resistor R , and there is no transient current on the output.

2.2.3 Series Resistance Compensation

The patch recording configuration provides a nearly ideal voltage clamp situation for single-channel currents. The series resistance (Pipette resistance plus any other access resistance to the patch or cell) to the membrane patch is typically 2-10 M ohm, and the patch capacitance is less than 0.1 pF, yielding a charging time constant of 1 μ sec or less. This is the time constant for charging the patch of membrane when a potential step is applied to the pipette, and it is also the time constant of the pipette current arising from a step change in patch current. The voltage errors are also very small: a 10-pA channel current causes a voltage drop of at most 0.1 mV in the series resistance (R_s).

The situation is very different in the case of whole-cell recording. Instead of the patch capacitance, the entire cell's membrane capacitance contributes to the charging time constant. For a spherical cell, the approximate membrane capacitance C_m (in pF) is related to the diameter d (in mm) by

$$C_m = \pi d^2 / 100$$

so that a 20 μm cell has a capacitance of 12 pF or more. The series resistance is often higher, typically 5-20 M ohm, so that time constants of several hundred microseconds are common. Voltage errors can also be considerable, since whole-cell currents larger than 1 nA are typical. These currents can cause errors of tens of millivolts in the measurement of the membrane potential.

Figure 5 shows the diagram of series resistance R_s compensation. A fraction of the current monitor signal is added to the command signal, giving positive feedback.

The command signal V_{cmd} (V_{ref}) is summed with the compensation signal to form the pipette potential V_p . This is filtered by the R_s and C_m , yielding V_m . The resulting pipette current is C_m times the time derivative of V_m . It is converted to a voltage by the I-V converter and associated circuit. This current monitor voltage is then scaled by a factor depending on R_s compensation resistor to form the compensation voltage. A fraction of the current monitor signal is added to the command signal, giving positive feedback to electronically reduce the effect of the series resistance.

2.3 Pipettes

The object of the patch current measurement is a small membrane patch and a pipette tip of comparable dimensions. Both are at the limit of resolution of the optical microscope. Only rarely is it possible to see the membrane patch during the experiment, and even then quantitative evaluation of its size is impossible or difficult. The conductance measured before the tip touches the cell membrane can provide an estimate of the pipette tip geometry.

Pipettes fabricated from commercially available soft glass were pulled by the two-stage procedure described by Hamill et al (1981). These pipettes have pipette resistances ranging from 1 M ohm to 5 M ohm when filled with pipette solution. The exact value is determined by the coil heat setting of the final pull.

The tip shape is approximately conical, with an angle ϕ of 24 degree for the average type of pipette when the pipette is modeled as having an approximately cylindrical shank and a conical tip. The total resistance of the pipette is given by the sum of the tip and the shank resistance

$$R = PL/\pi R_s^2 + (P \cot(\phi/2)/\pi)(1/R_t - 1/R_s)$$

P: resistivity of the solution in tube.

L: length of the tube

Since the radius of the cylindrical shank R_s is much larger than the radius of the tip opening R_t (Figure 6), the resistance of the tip dominates the total resistance of the pipette. The main limitations, in terms of voltage and background noise, is the series resistance located in the pipette tip. For whole cell recording the pipettes should be relatively wide and they should have a steep taper in order for us to reduce the series resistance of the pipette.

2.4 Enzymatic Dispersion of Heart Tissues

Enzymatic dispersion of the tissues is the isolation of single cell using enzymes. A large number of techniques have been developed for the enzymatic isolation of many types of cells since the first trials around 1970. Most of the procedures have been designed to meet the needs of biochemical

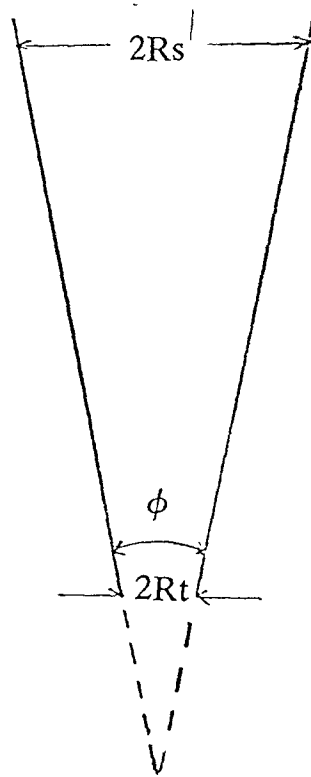


Figure 6 Outline of pipette

investigations. For electrophysiologists, enzymatic dissociation is of interest if the cells are not easily accessible otherwise or if they are coupled to a complex electrical network, for example, in the heart. Enzymatically isolated cells also turned out to be very well suited for the patch clamp technique. They have a cell surface stripped of connective tissue, a prerequisite for the formation of a gigaseal between the current recording pipette and the cell membrane.

The starting material for primary cell cultures is mostly obtained by enzymatic dissociation. Because of the complexity of cell links and the diversity of intercellular materials, a standard method for tissue dissociation does not exist. Different dissociation method must be applied to different tissues.

In spite of the diversity of specifications, many procedures for the isolation of single cells follow a common sequence of steps:

1. Washout of blood.
2. Digestion of enzymes: The connective tissue is usually dissolved by collagenase.
3. Mechanical agitation.
4. final cleaning: To stop the exposure of the cells to the enzymes, we often wash them with fresh solution without enzymes.

3 METHODS

3.1 Animal

Male normotensive wistarkyoto strain rats (WKY) were purchased from Taconic Farm, Inc., Germantown, NY. They were subjected to a 12 hour light/dark cycle with free access to food and water in the UMD Research Animal Care Facility for several days prior to experimental manipulations. All experiments were made on 10-11 week old rats with a body weight of 260-370 g.

3.2 Single-cell isolation

Single ventricular myocytes were isolated using a method similar to that of Yazawa Kaibara, Ohara and Kameyama (1990). Briefly, after an animal was anesthetized with sodium pentobarbital (50 mg/kg). The heart was removed and the aorta connected to a modified Langendorf system. The heart was then sequentially perfused (37 °C) with Tyrode solution (5 min), Ca²⁺-free Tyrode solution (5 min), Ca²⁺-free tyrode solution containing collagenase Type 1 (Sigma, 30-40 mg/30ml recirculated for 20-30 min) at a flow rate of 5-10 ml/min and a hydrostatic pressure of 70-80 cm H₂O. After these treatments, the heart was optimally digested, and then washed with "storage solution" (23 °C) for 5 min and the left ventricle cut into 3x3 mm pieces. 1 or 2 pieces were transferred to a small beaker, cut into finer pieces, and filtered through a 250 μm polypropylene mesh. After these steps, single cells are suspended in the solution. The purpose of this treatment is the isolation

of single cells for an easy formation of gigaseal contacts between the pipette and the membrane. The effluent containing myocytes was kept in the storage solution at 4 °C or room temperature.

3.3 Electrophysiological Recording

During the experiment a small volume (50-100 μm) of the above solution containing dissociated myocytes was pipetted into a chamber having a coverglass bottom and a volume of about 0.5 ml. Currents mediated by potassium channels were investigated with the whole-cell recording technique (Hamill, Marty, Neher, Sakmann and Sigworth, 1981). Recording pipettes were made from 1.5 mm o.d. glass tube (World Precision Instruments Inc., New Haven, CT) by a two-stage pull on a David Kopf (Model 700C) vertical puller. When filled with the pipette solution the resistance of such electrodes was 2-4 M Ω . Application of mild suction (0-30 cm H_2O) to the back of such a recording pipette gently pressed against a myocyte resulted in gigaseals of 10-20 G Ω . The pipette potential then records the negative voltage of the cell interior (70 mV below the bath potential), and a repetitive voltage step of a few millivolts amplitude is applied. At this stage, the fast capacitance compensation is adjusted to cancel the transient caused by the capacitance of the pipette wall. Pulses of suction are applied to the pipette interior until a sudden increase in the size of the capacitive transients is observed. This additional current reflects the contribution of the cell membrane to the pipette input capacitance following the destruction of the patch of membrane. This further suction was applied to achieve the whole cell recording configuration. Series resistance error was reduced by adjusting

the series resistance compensation of the recording amplifier. Once the whole cell recording mode is established, it is often helpful to lift the pipette somewhat to relieve the strain imposed on the cell when the initial seal was established. In some cases, the cell may be lifted further to detach it from the bottom of the recording chamber. In such cases, the solution surrounding the cell can then be changed rapidly. The cells were held at -80 mV (cell interior relative to outside). The potassium current was recorded by applying 0.2-second-long depolarizing pulses from a holding potential of -80 mV and voltage-clamp protocols (Magnitude and length of these protocol are shown in each figures) applied with an Axopatch-1D amplifier and Pclamp software (Axon Instruments Inc. Burlingame, CA). All experiments were performed at a room temperature of 22-23 °C and the bath was perfused continuously with control (without drug) or drug containing bath solution at rates of 2-3 mL/min. We can know what we recorded is potassium current because the bath solution and the pipette solution are selected specially for recording of potassium current.

3.4 Solution

The following solutions were bubbled with 100% oxygen before and during perfusion of the heart or the tissue chamber. Each solution had a measured osmolality of 290-310 mOsmoles/ kg and contained the ingredients indicated in mM.

Tyrode Solution: NaCl 135, KCl 5.4, CaCl₂ 1.8, MgCl₂ 3, NaH₂PO₄ 0.25, HEPES 10, glucose 10, pH 7.3 with NaOH. Pipette Solution: KCl 50, K glutamate 60, MgCl₂ 3, CaCl₂ 1, HEPES 10, EGTA 11,

K₂ATP 5, pH 7.3 with KOH.

Bath Solution: Tris.HCl 140, Tris.base 20, KCl 4.8, MgCl₂ 3, CaCl₂ 0.1, CdCl₂ 0.2, dextrose 10, pH 7.3 with KOH.

Storage Solution: L-glutamic acid 50, KCl 40, Taurine 20, KH₂PO₄ 20, MgCl₂ 3, glucose 10, HEPES 10, EGTA 0.5, pH 7.4 with KOH.

3.5 Cell Capacity and Series Resistance

The capacity transient due to the recording pipette was initially corrected for in the cell attached mode (the state of pipette and membrane attached) with the capacitance compensation controls of the amplifier (adjust R₂ and C₂ in Fig.2). The membrane patch was then ruptured with additional suction in order to form the whole-cell recording configuration. Prior to further compensating for membrane capacitance and series resistance, a 10 mV hyperpolarizing step pulse from a holding potential of -80 mv was applied and the current response recorded (figure 7). This was repeated after analogue correction was made for the cell capacitance and series resistance. The capacity (C_m) was then calculated according to the equation

$$C_m = Q/V$$

where Q is the area under the current transient (total charge, integrated by using the pClamp-clampan program) and V is the magnitude of the hyperpolarizing step (10 mV). The decay of the capacitance transient was fitted with the single exponential function

$$Y_t = A_0 \exp(-t/T)$$

where T is the membrane time constant. Series resistance was then calculated from the expression

X2429C08 0: 0: 41

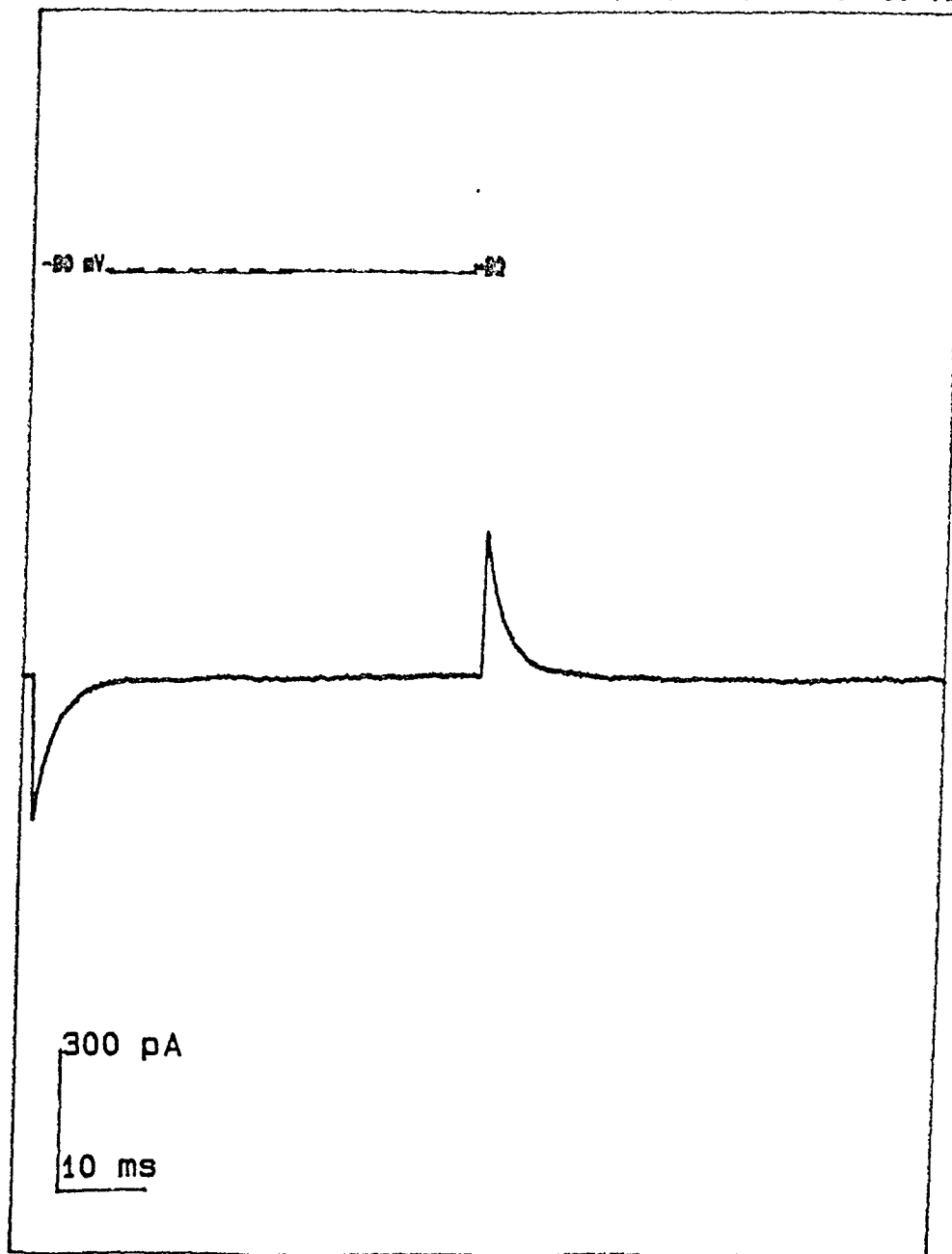


Figure 7 Current activated in a 10 mV hyperpolarizing pulse from a holding potential of -80 mV

$$R_s = T/C_m$$

Decay time constants for potassium currents were determined by least squares fitting of the one-exponential function

$$I_t = A_0 + A_1 \exp(-t/T_1)$$

to the current trace. A_0 is the initial current amplitude, and A_1 is the extrapolated maxima of the decaying components. T_1 is the decay time constant for potassium current.

3.6 Voltage Protocols and Analysis of Membrane Current

Current recordings were obtained using the whole-cell voltage clamp method using an Axopatch-1D amplifier. Records were acquired using a pClamp data acquisition and analysis program and stored on an IBM-compatible microcomputer.

All of the results illustrated in the figures are representative of at least three complete experiments of the same design .

For most experiments, brief voltage steps were applied from the holding potential. Control data were taken 5 minutes after changing to the appropriate extracellular bath solution. The bath was then changed to BDM-containing bath solution using continuous perfusion, and the currents were measured 5-10 minutes later. The bath was then changed back to drug-free solution and protocols were repeated 5-10 minutes after washout.

4 RESULTS

Figure 8 shows records of ionic currents that can be recorded from rat ventricular myocytes from a holding potential of -80 mV in normal bath solution. It shows the membrane current activated in 10-mV increments from -80 mV to +60 mV. Depolarizing clamp pulses positive to -60 mV activated the fast sodium current (occured in the first 3 ms, which is hard to see in the figures) which at positive potentials was followed by a transient outward potassium current, the predominant outward current in rat ventricular myocytes. Figure 9 shows that when the myocytes were exposed to 20 mM BDM, the inactivation of outward transient potassium current was accelerated and the steady-state current was reduced. The initial outward peak current was suppressed relatively little at first (when the drug was just put in), but eventually decreased as the full effect of the drug was reached in 3 to 5 minutes. The acceleration of inactivation induced by BDM was present at all membrane potentials such that the outward transient current inactivated almost completely within 30 msec as compare with 100 msec measured in control solution. Figure 10 shows that when the myocytes were exposed to 50 mM BDM, the inactivation of outward transient potassium current was accelerated further and the steady-state current was reduced lower than that in figure 9 (20 mM BDM).

We can see from this that the superfusion of myocytes with BDM elicited a dose dependent decrease of outward transient potassium current.

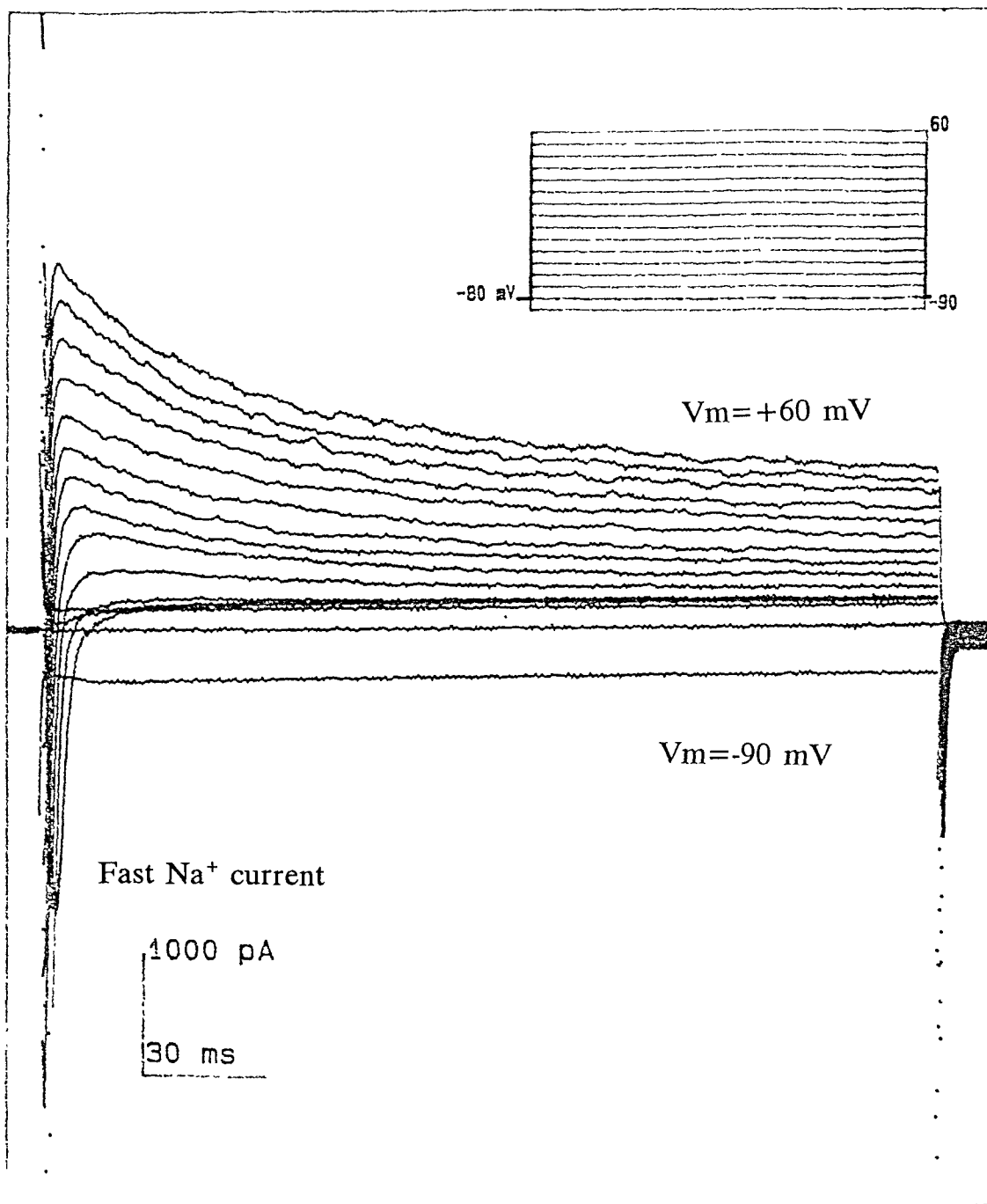


Figure 8 Outward transient potassium current activated in 10 mV increments from -80 to 60 mV in normal bath solution

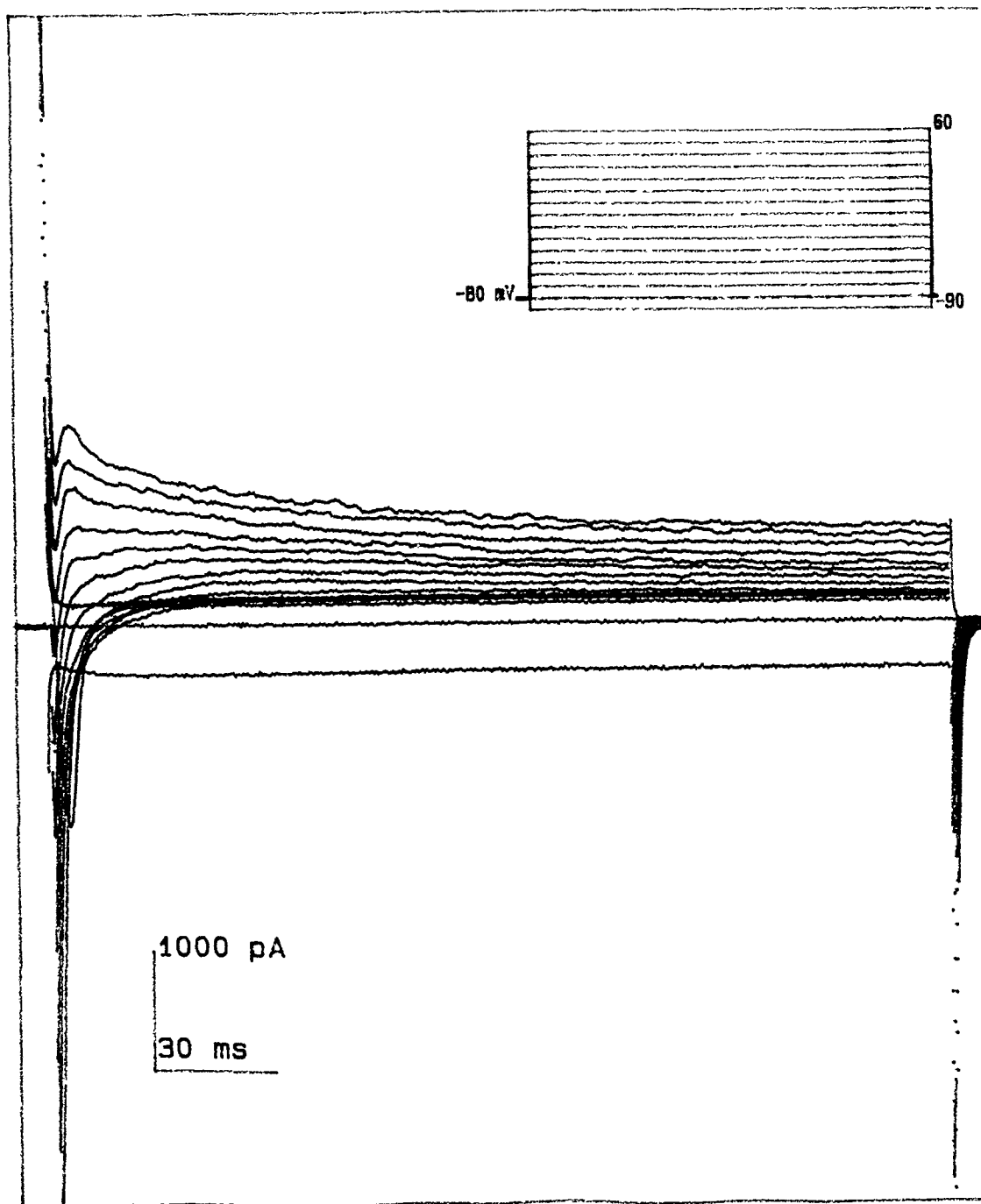


Figure 9 Outward transient potassium current activated in 10 mV increments from -80 to 60 mV after 10 min wash-in of 20 mM of BDM

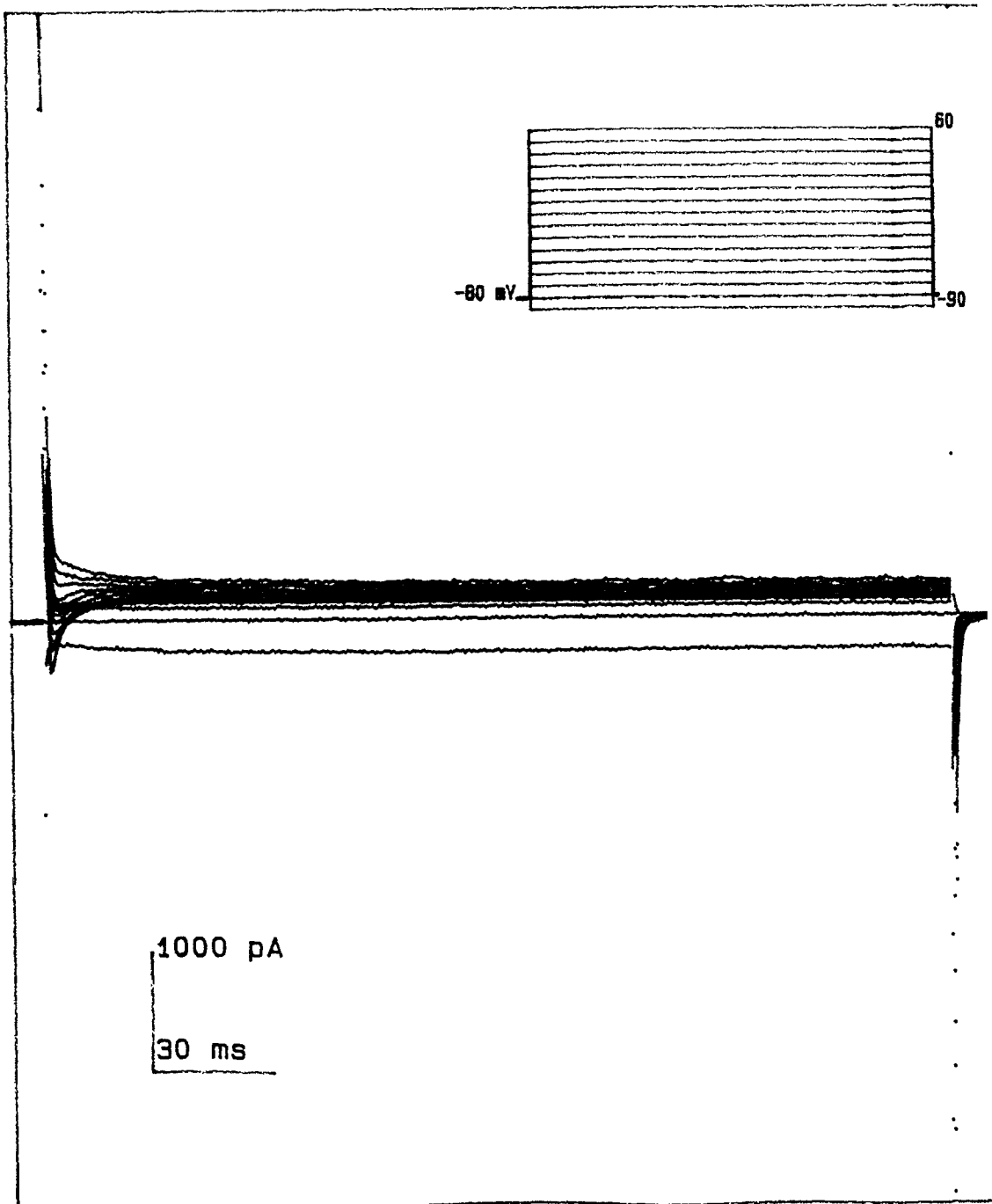


Figure 10 Outward transient potassium current activated in 10 mV increments from -80 to 60 mV after 10 min Wash-in of 50 mM of BDM

BDM with concentrations of 5, 20 and 50 mM reduced the maximal peak outward transient potassium current (voltage step from membrane holding potential -80 mV to +60 mV) by $7.3\pm 3.2\%$, $68.7\pm 6.1\%$ and 100%. The steady-state level is also reduced. Figure 11 shows that the outward transient potassium current recovered slowly upon washout regaining 70% of its control value in 8 to 10 minutes.

Experiments of the type illustrated in figures 8 to 11 were performed routinely with 20 and 50 mM BDM. Under control condition outward transient potassium current at +60 mV had an initial value of 2868.7 ± 4.3 pA ($n=3$) and declined by $81.1\pm 1.3\%$ to a final steady current of 678.2 ± 2.1 pA with a single time constant. The addition of 20 mM BDM suppressed the final current by $65.1\pm 2.3\%$ and the time constant of its inactivation by $83.5\pm 3.0\%$.

Figure 12 shows the effect of 50 mM BDM on the voltage dependence of the initial peak (circles) and steady-state (triangles) components of outward transient potassium current. Figure 13 shows the effect of BDM on its time constant of inactivation. Both the initial and final values of outward transient potassium current increased linearly with potential. BDM suppressed the final current (filled triangles) by roughly the same fraction at all positive potentials. The time constant of inactivation, measured from 0 to 50 mV, was reduced by BDM from 39.2 ± 3.2 msec to 5.2 ± 1.1 msec although it was insensitive to potential both before and after the addition of the drug.

Figure 14 and Figure 15 show that $5\ \mu\text{M}$ of isoproterenol (Iso) increased the peak of outward transient potassium current and the steady-state level by

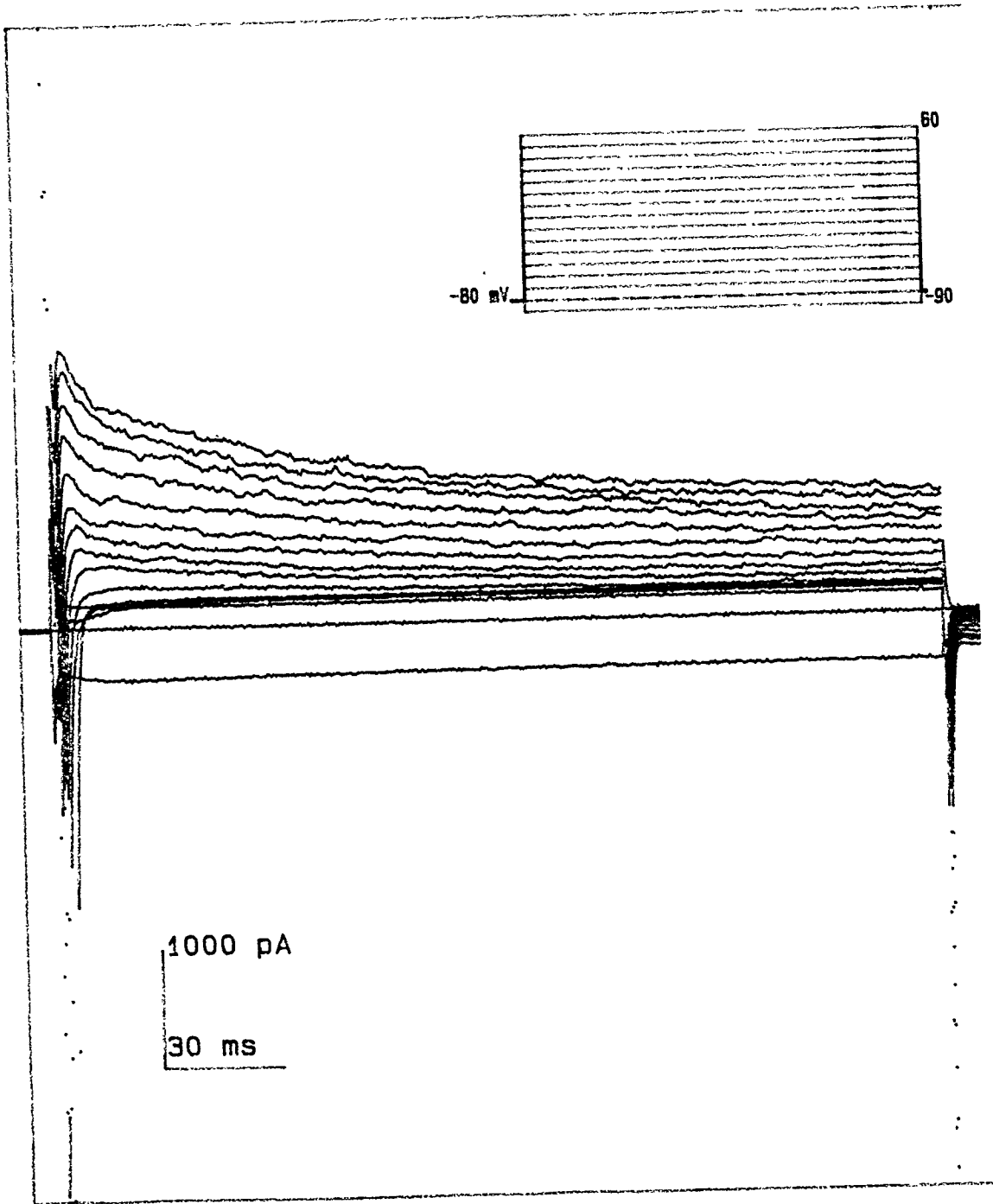


figure 11 Washout current records

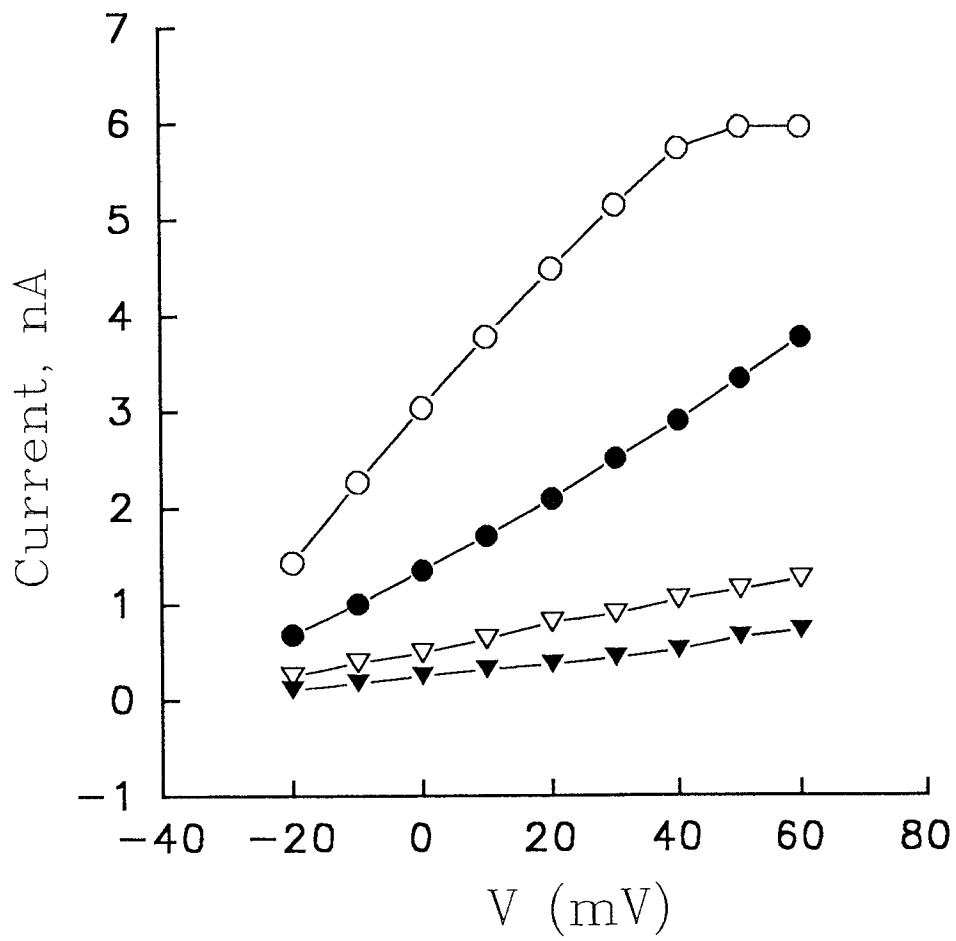


Figure 12 Voltage dependence of outward transient potassium current in the absence and presence of 20 mM BDM

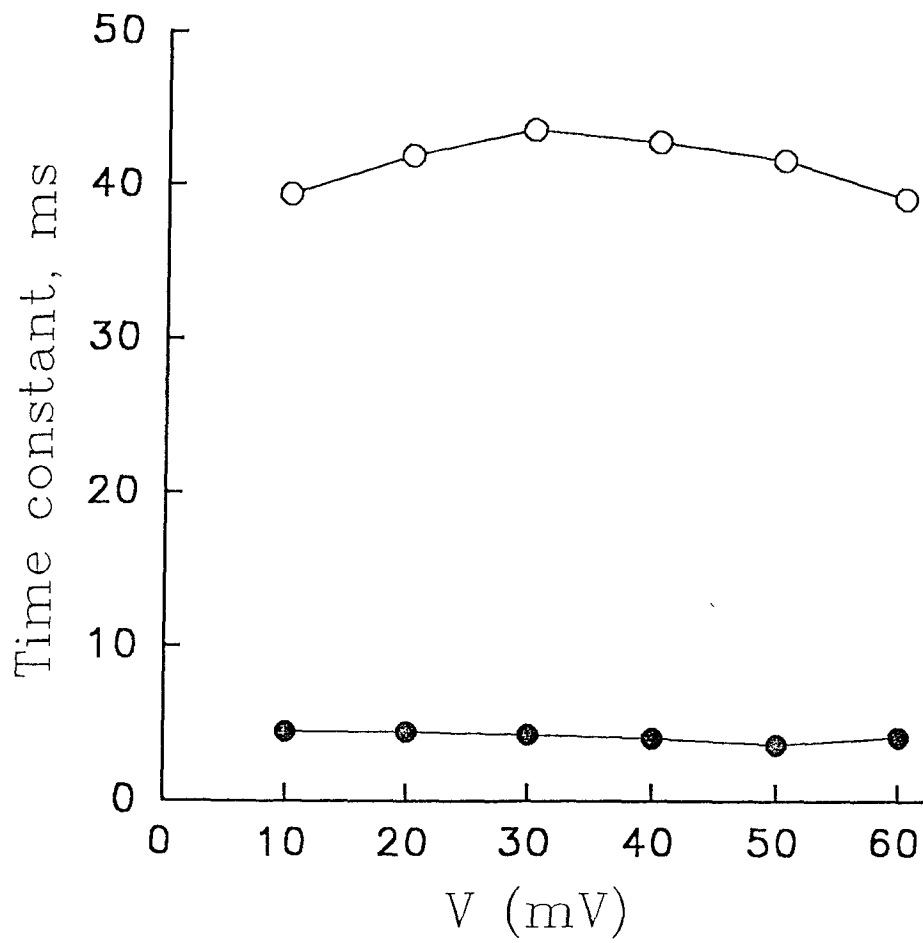


Figure 13 The time constant curve in the absence and presence of 20 mM BDM

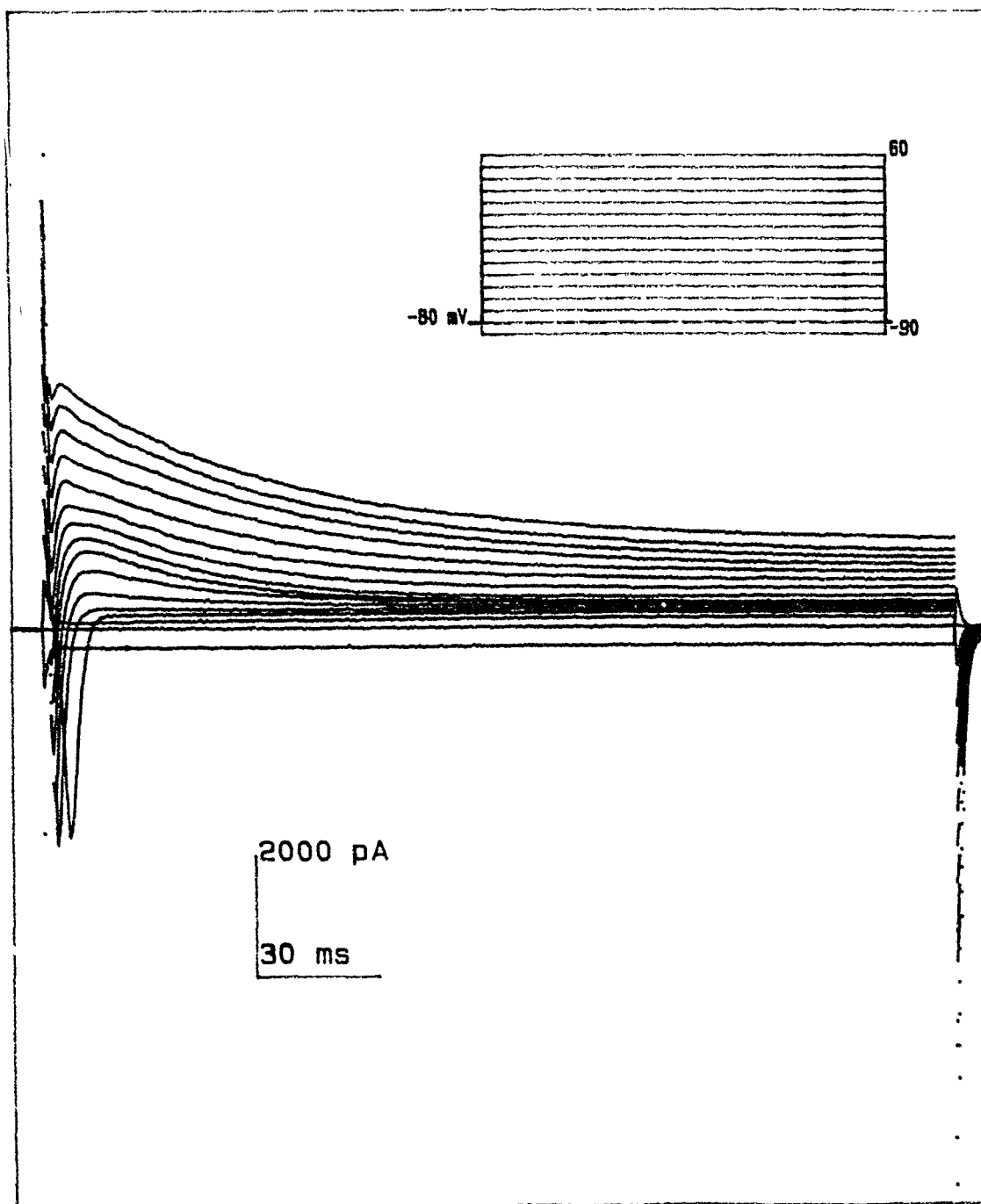


Figure 14 Membrane current activated in 10 mV increments from -80 to 60 mV in normal bath solution

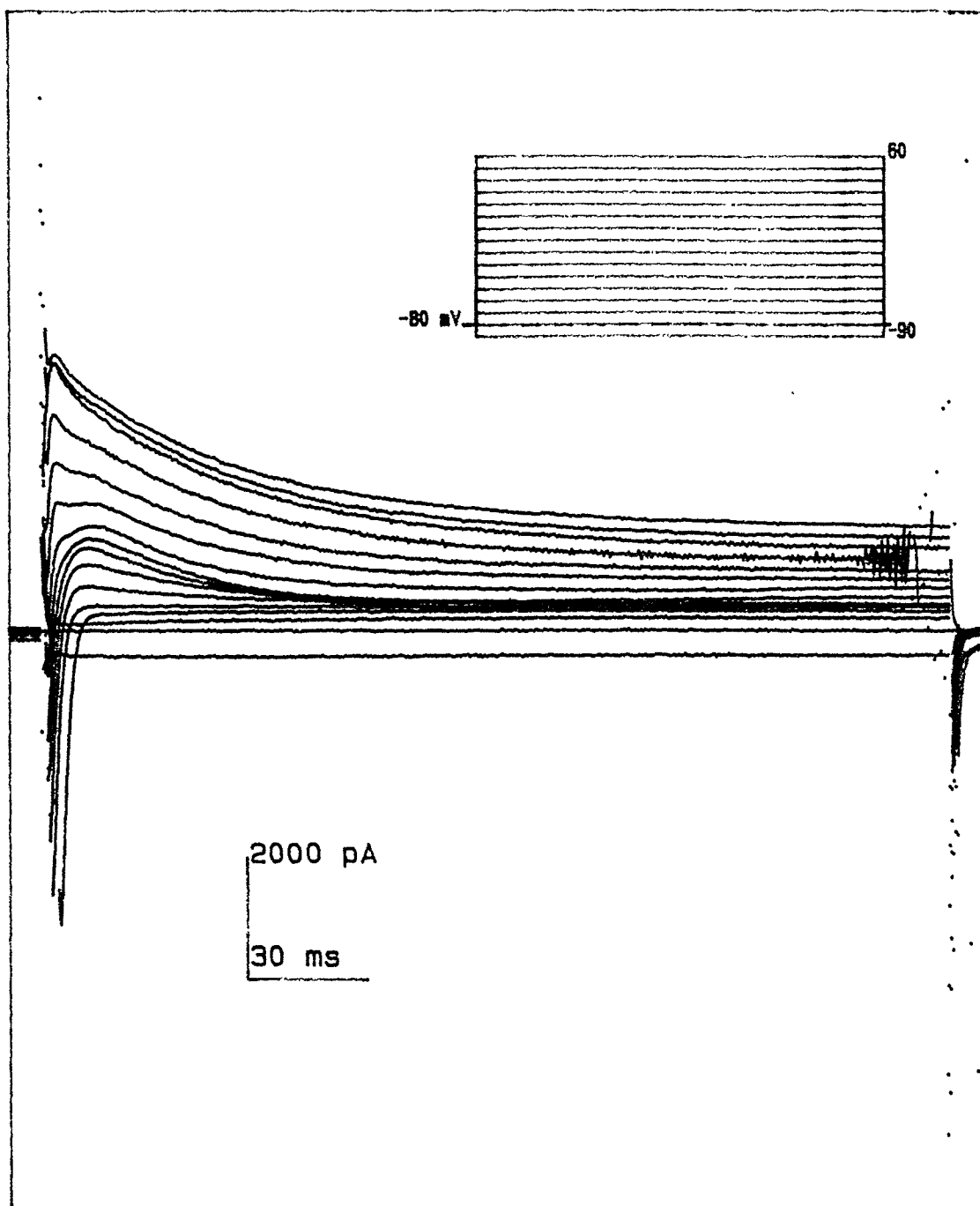


Figure 15 Membrane current activated in 10 mV increments from -80 to 60 mV after 10 min wash-in of 5 μ M of Iso

about 15%. Figure 16 shows that 5 μ M of Iso partially reversed the inhibitory action of 20 mM BDM on outward transient potassium current. Figure 17 shows that concentration of BDM above 5 mM caused a significant reduction in outward transient potassium current. The suppressive effect of BDM was found to be virtually complete at 50 mM of BDM.

Figure 18 is the dose-dependent curve of the effect of BDM on the peak of outward transient potassium current (open circle) and steady-state current (filled circle). Figure 19 is the time-constant of the inactivation current curve. We can see that when the concentration of BDM increases the time-constant of inactivation becomes smaller.

The possible voltage dependence of the BDM block of the outward transient potassium current channel was investigated in a number of ways:

(1) The time constant of the inactivation process of outward transient potassium current was measured at various pulse potentials as indicated in figure 13. Using the curve fitting program, it was found that the inactivation process was well-fitted by one exponential.

(2) Evaluation of net potassium efflux by measurement of the peak of outward transient potassium current and the steady-state level.

BDM failed to modify the voltage dependence of the steady-state inactivation of outward transient potassium current. This was measured using test potentials of +60 mV with 500 msec conditioning holding potentials ranging between -90 mV and 0 mV. Figure 20, Figure 21 and Figure 22 show that the control steady-state inactivation of outward transient potassium current shows a steep voltage dependence in the range of -70 mV to -50

mV. 20 mM BDM failed to alter this relationship, suggesting that the drug did not affect the voltage gated parameters of outward transient potassium current.

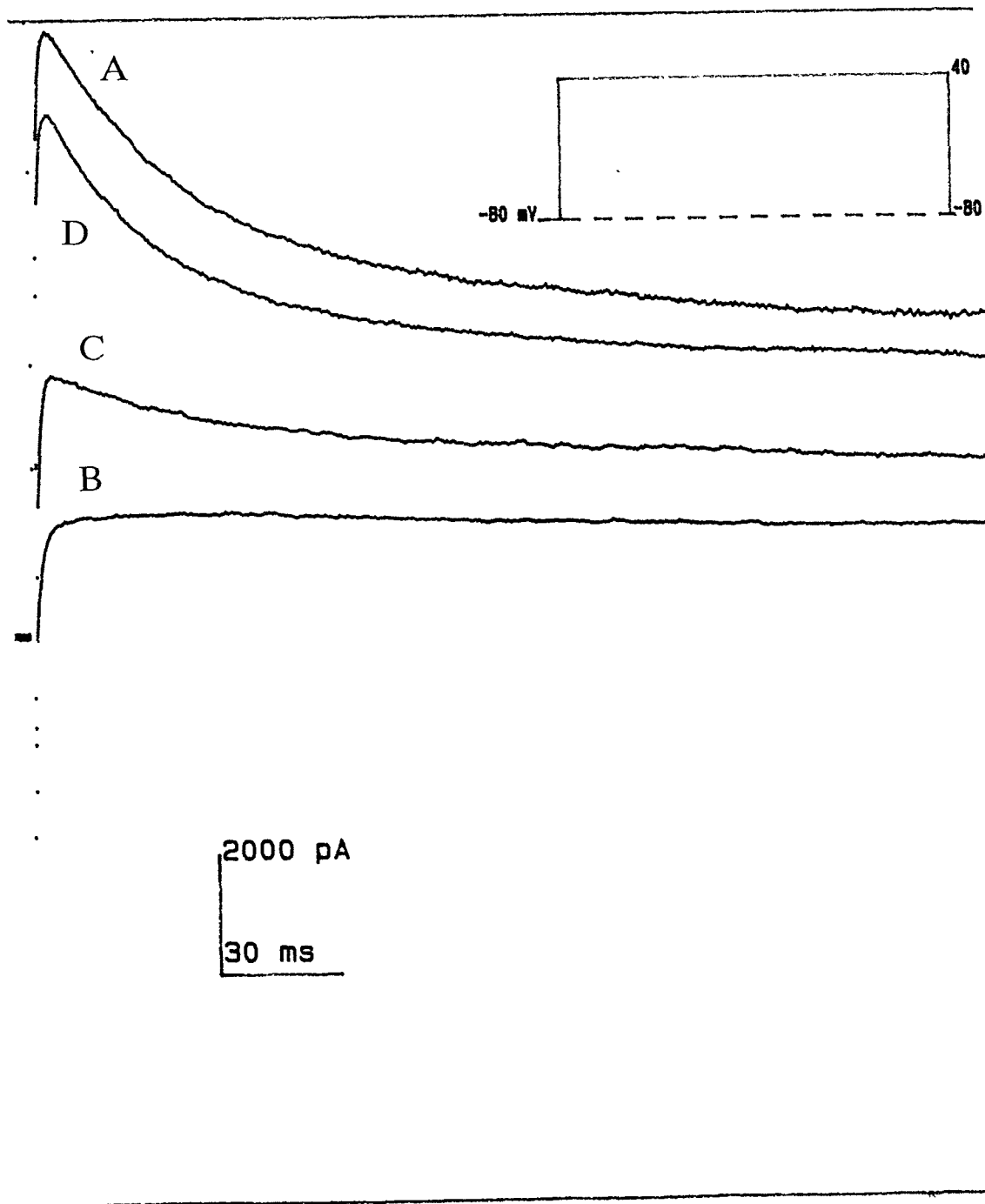


Figure 16 Partial reversal effect of Iso

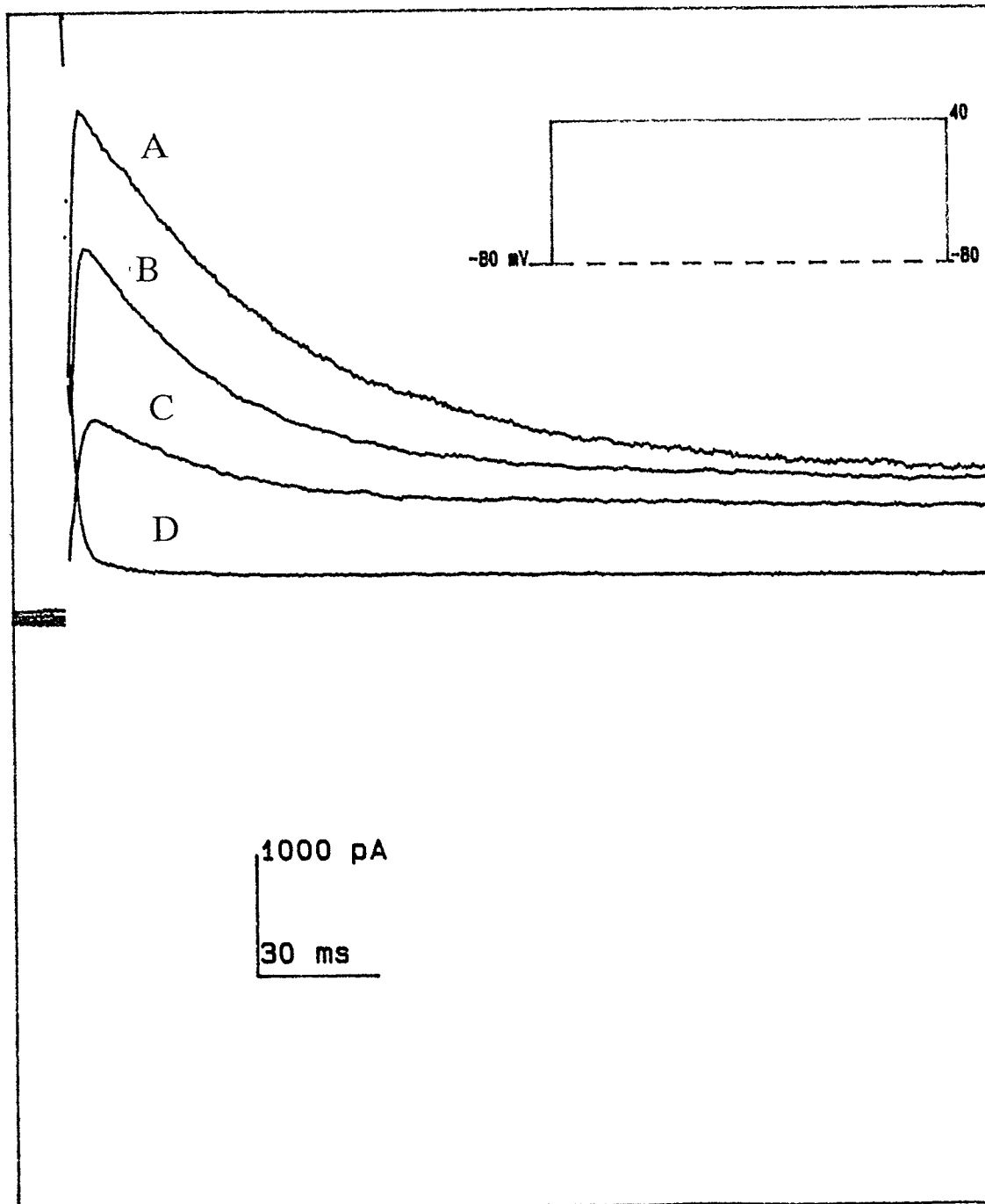


Figure 17 BDM dose-dependent curve

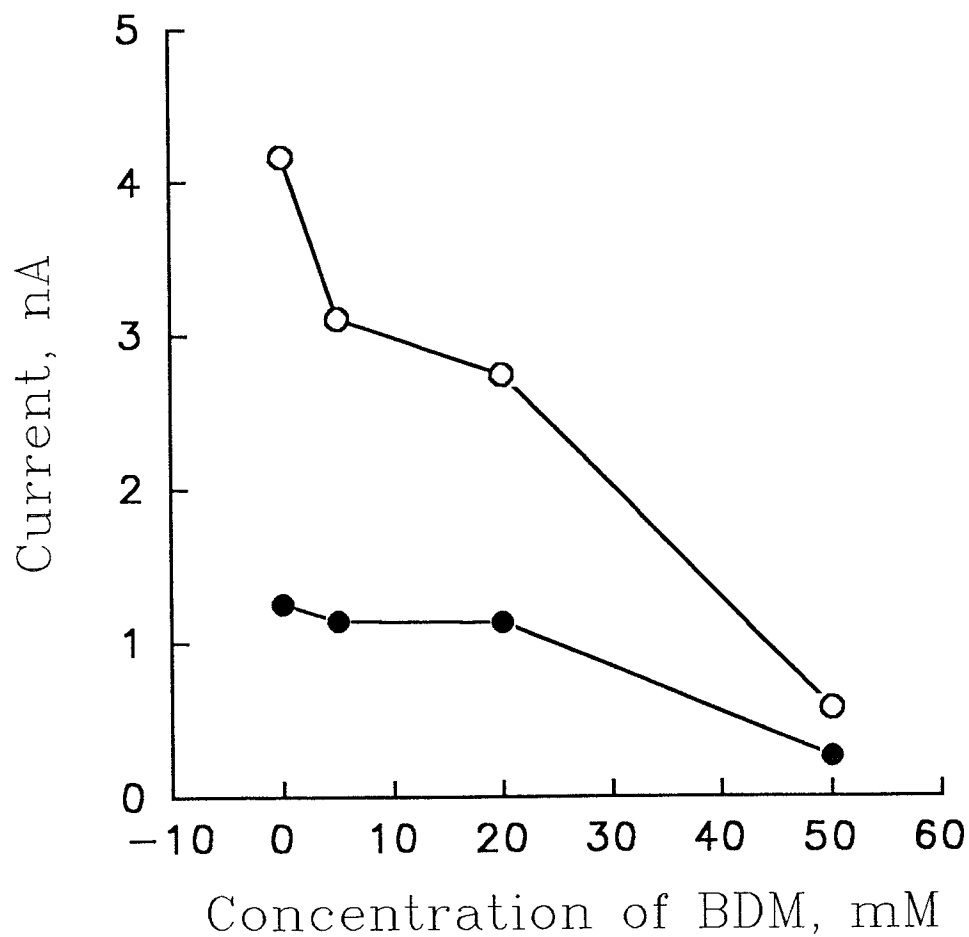


Figure 18 Dose-dependent curve of the effect of BDM on the peak current and steady-state current

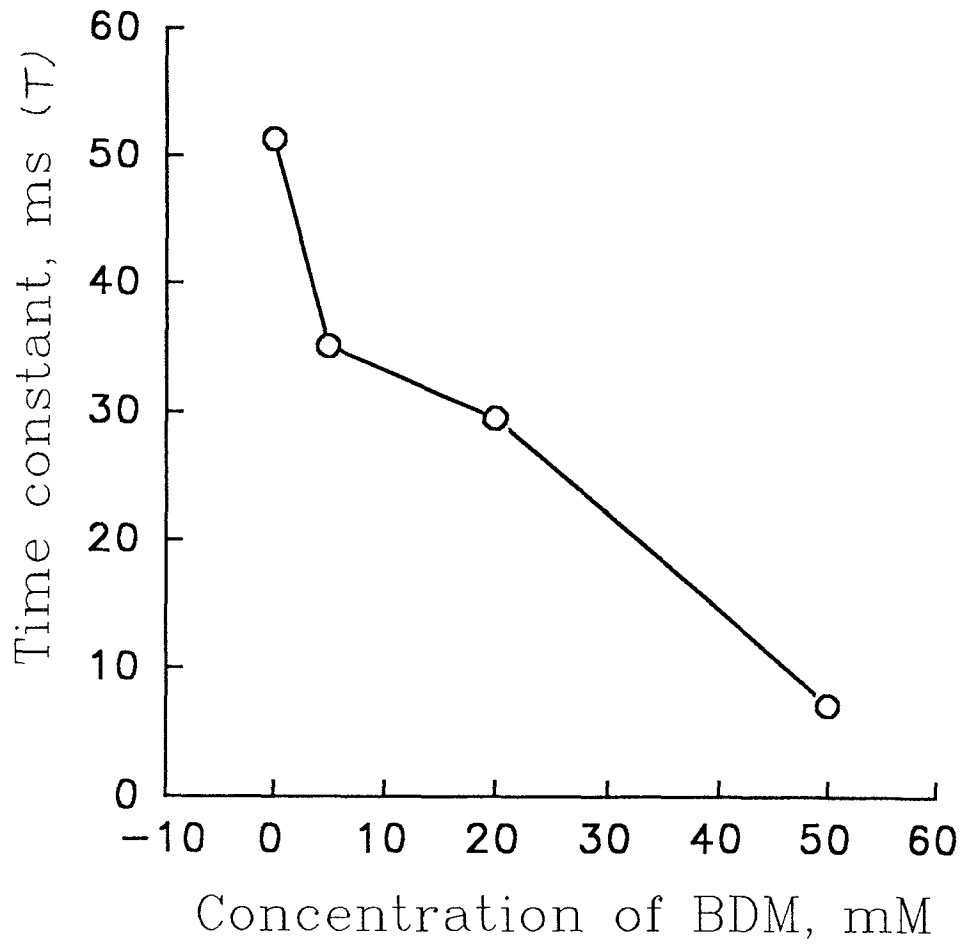


Figure 19 Dose-dependent curve of the effect of BDM on the single exponential time of decay rate

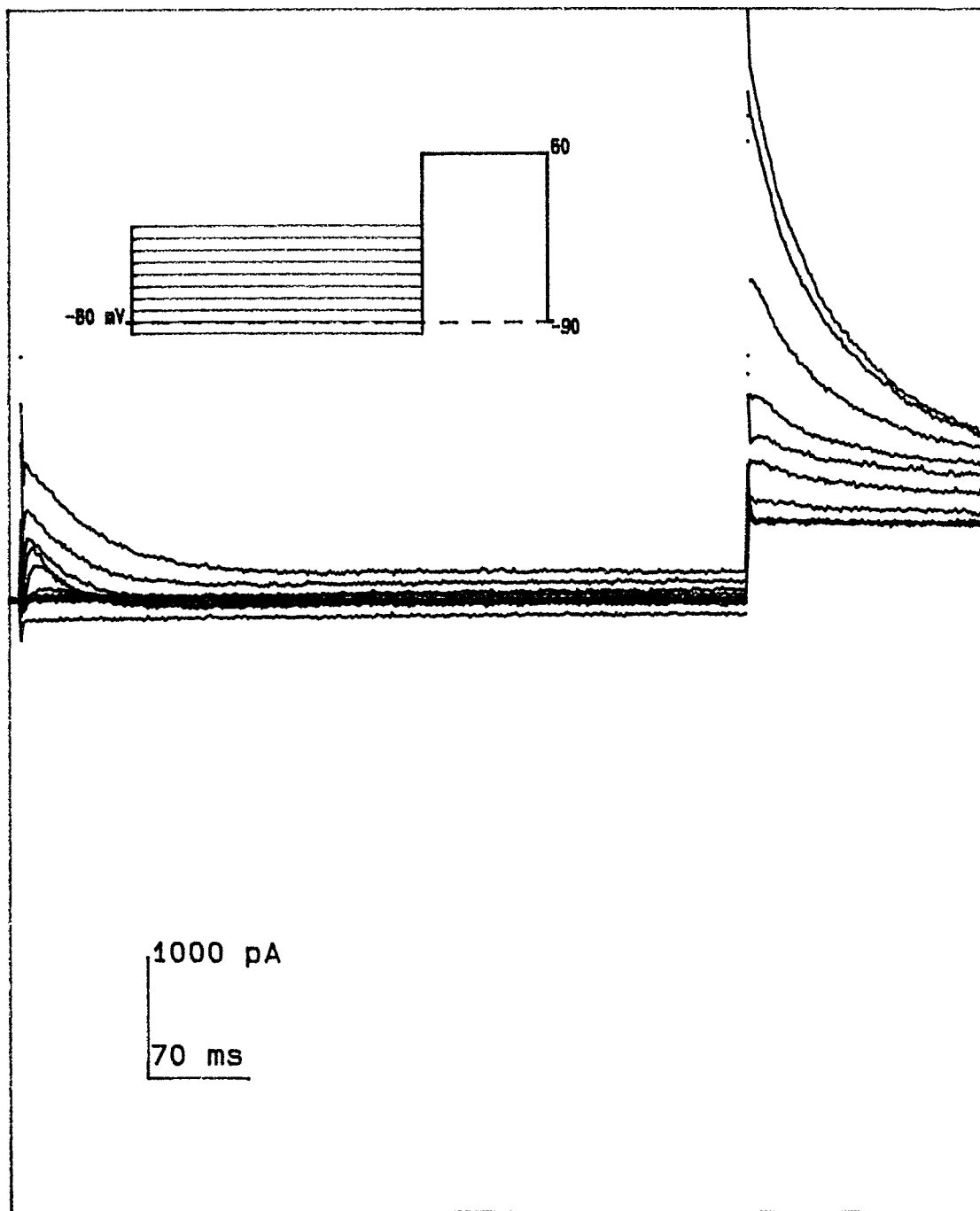


Figure 20 Inactivation curve of outward transient potassium current examined in the absence of BDM

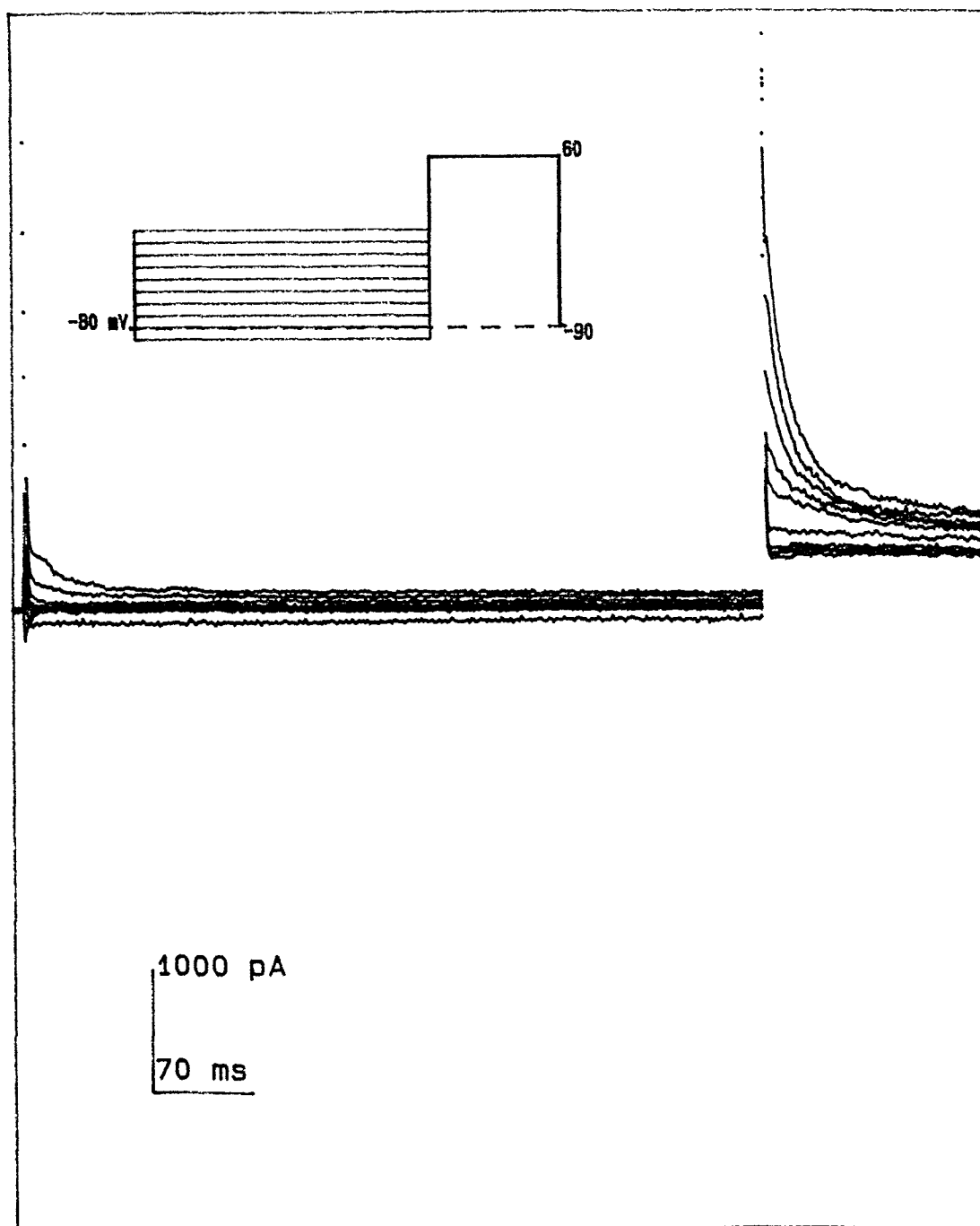


Figure 21 Inactivation curve of membrane current examined in the presence of 20 mM BDM

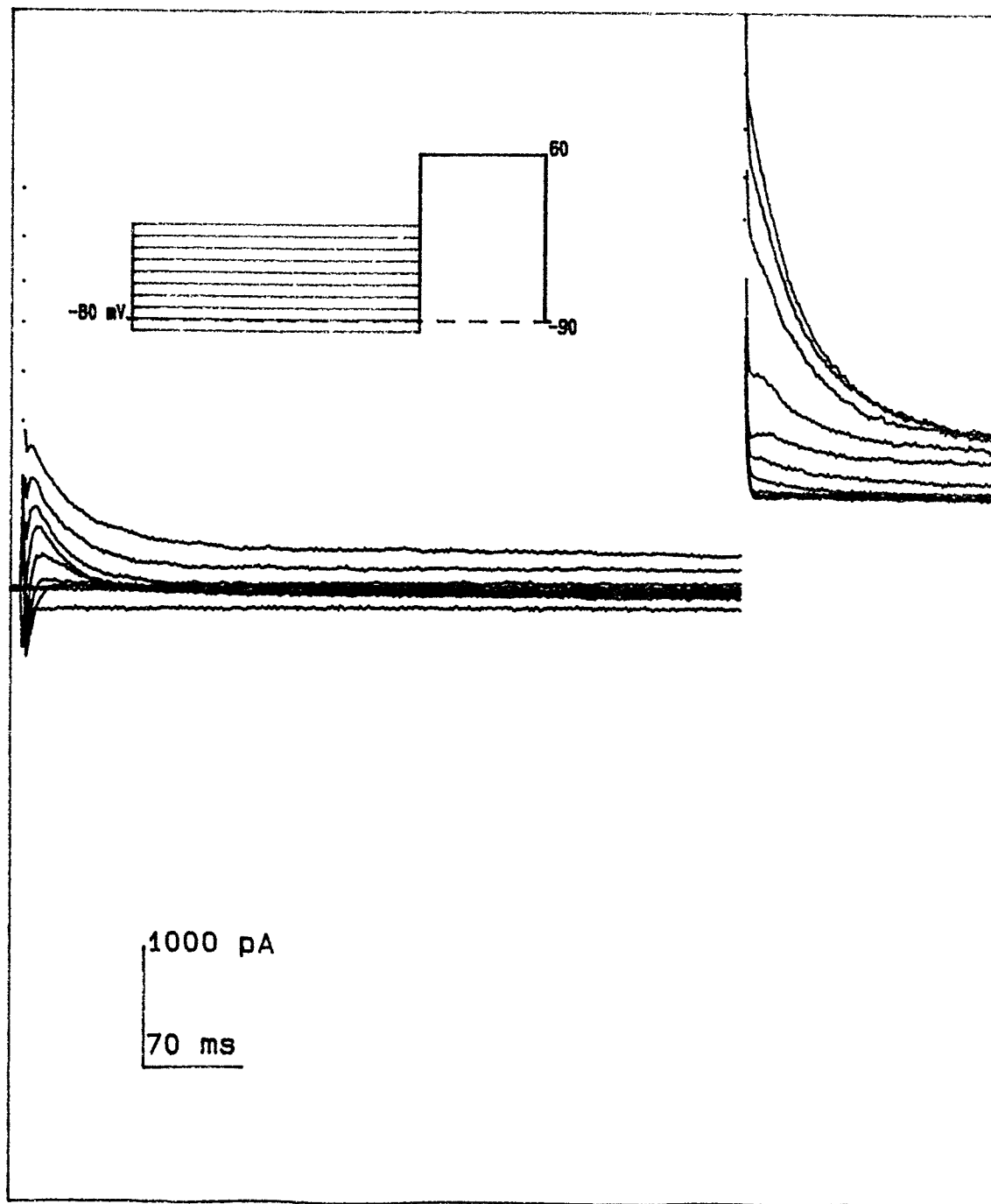


Figure 22 Inactivation curve of membrane current examined after 10 min of normal bath solution

5 DISSCUSSION AND CONCLUSION

The potassium current in rat ventricular myocytes was studied using BDM under voltage clamp conditions. At concentrations of BDM in the bath solution ranging from 5 to 50 mM a dose-dependent increase in the speed of inactivation of the outward transient potassium current was recorded. BDM blocked the rapidly activating potassium current by a process resembling accelerated inactivation and had no effect on the voltage dependence of steady-state inactivation of outward transient potassium current. These findings suggest that BDM blocks the potassium currents by binding relatively slowly to the inner aspect of the potassium channel only when it is in the open state. We also tried isoproterenol (Iso) and found that it reversed the blocking effect of BDM. The present data suggest that BDM and Iso can either inhibit or enhance respectively the outward transient potassium current by dephosphorylation or phosphorylation of the channel proteins, respectively. Based on this mode of action one would predict that BDM does not alter the single channel conductance but reduces the interval during which a single channel is open.

Our results clearly show that BDM enhances the apparent inactivating kinetics of cardiac outward transient potassium current. This was reflected by an increases in the rate constant of the inactivation process as well as a decreases in the total efflux of potassium through the potassium channels concerned.

Since outward transient potassium current has been characterized in pacemaking cells as the predominant outward current, it seems safe to speculate that the bradycardic effect of BDM are mediated by the modulation of an outward transient potassium current. Since the duration of the action potential plateau is in part regulated by the modulation of potassium current, it is reasonable to hypothesize that the effect of BDM on potassium current may prolong the duration of action potential. Since prolongation of the cardiac action potential has long been recognized as a potent antiarrhythmic mechanism (Vaughan Williams, 1984), the effect of BDM on potassium current may be the cause of the antiarrhythmic effects of the drug. In this respect, it should be noted that outward transient potassium current also has been found in human cardiac atrial tissue (Escande et al, 1987), which may render this drug useful as an antiarrhythmic agent.

Combined with the previous data, it is suggested that BDM can nonselectively inhibit potassium and calcium channels by dephosphorylation of the channels.

REFERENCES

1. Agus, Z. S., Dukes, I. D. and Morad, M. "Divalent Modulate Transient Outward Current in Isolated Rat Ventricular Myocytes." *J. Physiol.* 418 (1989): 28-30.
2. Agus, Z. S., Kelepouris, E. L., Dukes I. D. and Morad, M. "Cytosolic Magnesium Modulates Calcium Channel Activity in Mammalian Ventricular Cells." *Am. J. Physiol.* 256 (1989): 452-455.
3. Aldrich, R. W. "Inactivation of Voltage Gated Delayed Potassium Current in Molluscan Neurons. A Kinetic Model." *Biophys. J.* 36 (1981): 519-532.
4. Boyett, H. R. "A Study of the Effect of the Rate of Stimulation in the Transient Outward Current in Sheep Cardiac Purkinje Fibres." *J. Physiol. Lond.* 319 (1981): 1-22.
5. Clark, R. B., Giles, W. R. and Imaizumi, Y. "Properties of the Transient Outward Current in Rabbit Atrial Cells." *J. Physiol.* 405 (1988): 147-168.
6. Dukes, I. D. and Morad, M. "Analysis of the Transient Outward Current in Isolated Rat Ventricular Cells." *Biophys.J.* 51 (1987): 412-413.
7. Escande, D., Coulomee, A., Faivre, J. Deroubaix, E. and Coraboeuf, E. "Two Types of Transient Outward Currents in Adult Human Atrial Cells." *Am. J. Physiol.* 252 (1987): 142-148.
8. Fryer, M. W., Neering, I. R. and Stephenson, D. G. "Effects of 2,3-Butanedione Monoxime on the Contractile Activation Properties of Fast-and Slow-Twitch Rat Muscle Fibres." *J. of Physiol.* 407 (1988): 53-75.
9. Giles, W. R. and Van Ginneken, A. C. G. "A Transient Outward Current in Isolated Cells From the Crista Terminalis of Rabbit Heart." *J. Physiol.* 368 (1985): 243-264.
10. Hamill, O. P., Marty, A., Neher, E., Salmann, B. and Sigworth, F. J. "Improved Patch-clamp Techniques for High Resolution Current Recording From Cells and Cell-free Membrane Patches." *Pfluegers arch.* 391 (1981): 85-100.

11. Harvy, R. S. and Hume, J. R. "Autonomic Regulation of a Chloride Current in Heart." *Science (Wash.DC)* 244 (1989): 983-985.
12. Jewell, B. "Rate Dependent Control of Action Potential Duration." *Progr. Biophys. Mol. Biol.* 15(1981): 125-179.
13. Josephson, I. R., Sanchez-Chapula, J. and Brown, A. M. "Early outward current in rat ventricular cells." *Circ. Res.* 54 (1984): 157-162.
14. Lang, R. J and Wendt, I. R. "Effect of 2,3-Butanedione Monoxime on Barium Currents Recorded in Single Smooth Muscle Cells of the Guinea Pig Ureter." *Proceedings of the Australian Physiological and Pharmacological Society* 18 (1983): 34-42.
15. Mitra, R. and Morad, M. "A Uniform Enzymatic Method for the Dissociation of Myocytes From Heart and Stomach of Vertebrates." *Am. J. Physiol.* 249 (1985): 1056-1060.
16. Oexle, B., Weirich, J. and Antoni, H. "Electrophysiological Profile of Tedisamil, a New Bradycardic Agent." *J. Mol.Cell. Cardiol.* 19:suppl.III (1987): 194-195.
17. Ohta, M. and Narahashi, T. "Sparteine Interaction With Nerve Membrane Potassium Conductance." *J. Pharmacol. Exp. Ther.* 187 (1973): 47-55.
18. Takumi, T., Ohkubo, H. and Nakanishi, S. "Cloning of a Membrane Protein that Includes a Slow Voltage-gated Potassium Current." *Science (Wash. DC)* 242 (1988): 1042-1045.
19. Tsang, G. and Hoffman, B. F. "Two Components of Transient Outward Current in Canine Ventricular Myocytes." *Circ. Res.* 64 (1989): 633-647.
20. Walsh, R. B. and Kass, R. S. "Regulation of a Heart Potassium Channel by Protein Kinase A and C." *Science (Wash. DC)* 242 (1988): 67-69.